Microscopic theory for the incommensurate transition in TiOCl

Diego Mastrogiuseppe and Ariel Dobry
Facultad de Ciencias Exactas Ingeniería y Agrimensura, Universidad Nacional de Rosario and Instituto de Física Rosario, Bv. 27 de Febrero 210 bis, 2000 Rosario, Argentina

(Received 18 March 2009; revised manuscript received 3 April 2009; published 24 April 2009)

We propose a microscopic mechanism for the incommensurate phase in TiOX compounds. The model includes the antiferromagnetic chains of Ti ions immersed in the phonon bath of the bilayer structure. Making use of the Cross-Fisher theory, we show that the geometrically frustrated character of the lattice is responsible for the structural instability which leads the chains to an incommensurate phase without an applied magnetic field. In the case of TiOCl, we show that our model is consistent with the measured phonon frequencies at $T=300$ K and the value of the incommensuration vector at the transition temperature. Moreover, we find that the dynamical structure factor shows a progressive softening of an incommensurate phonon near the zone boundary as the temperature decreases. This softening is accompanied by a broadening of the peak which gets asymmetrical as well when going toward the transition temperature. These features are in agreement with the experimental inelastic x-ray measurements.

DOI: 10.1103/PhysRevB.79.134430 PACS number(s): 63.20.kk, 75.10.Pq, 75.50.Ee

I. INTRODUCTION

In 1955, while writing an introductory solid-state textbook, Peierls[1] discovered that no one-dimensional (1D) metal could exist due to the electron-phonon coupling. Indeed, a half-filled metal is unstable toward a lattice dimerization. The system undergoes a metal-insulator transition because the loss of elastic energy is made up for by the electronic energy acquired when the gap is opened. A quite similar process takes place in a one-dimensional antiferromagnet, giving rise to the so-called spin-Peierls (SP) transition.[2] The lattice dimerizes and the antiferromagnetic quasi-long-range order is replaced by a gapped singlet state. From this point of view, no one-dimensional antiferromagnetic system should be stable.

In spite of this general prediction, only few spin-Peierls materials were found. Most of them were observed in the early 1970s in some organic charge-transfer systems. However, direct spectral characterization was lacking due to the unavailability of large crystals for inelastic-neutron-scattering measurements. In this context the discovery of $CuGeO_3$ in 1993, the first inorganic spin-Peierls system, renewed the interest in this subject. Large enough crystalline samples of $CuGeO_3$ could be obtained to undertake a detailed spectral characterization. An important conclusion of these studies was that in $CuGeO_3$, the nonadiabatic character of the phonons[3] is so important that the SP transition is not driven by a softening of a precursive phonon mode. It has been shown that an extension of the canonical theory of Cross and Fisher[4] could explain this feature.[5] Moreover, the dispersion relation of the phonons in the direction perpendicular to the magnetic chains should be taken into account in a nonadiabatic SP system such as $CuGeO_3$.[6]

The recent discovery of a spin-Peierls transition in the TiOX (X=Cl,Br) family has opened new questions about this spin-Peierls paradigm. The essential building blocks of these compounds are bilayer structures of magnetically active Ti ions connected by O ones. The position of a Ti ion in a layer is shifted with respect to the other in the neighboring layer, forming something like an anisotropic triangular structure. In fact TiOCl was initially thought to be a candidate for a *resonating valence-bond* state,[7] but it has been found to be mainly a one-dimensional magnetic system[8] with the Ti d_{xy} orbitals pointing toward each other in the crystallographic b direction.[9] The high-temperature magnetic susceptibility is well described by the Bonner-Fisher curve, indicating a nearest-neighbor magnetic exchange $J\sim 660$ K.[9]

The phase diagram of TiOCl does not correspond to a canonical SP system in the sense that an incommensurate intermediate phase appears between the high-temperature uniform phase and the low-T dimerized phase.[9,10] The transition temperatures are found to be $T_{c1}\sim 66$ K and $T_{c2}\sim 92$ K. In Ref. 10 a very large energy gap of about 430 K in the low-temperature phase and a pseudo-spin-gap below 135 K were also reported. The order of both transitions is still under debate.[11–13]

The origin of the intermediate phase is controversial and not yet well understood. As the position of a Ti ion in a chain is shifted with respect to another one in the neighboring chain, it is plausible to speculate that some type of competition between the in-chain and out-of-chain interactions could be the origin of the incommensurate phase. This was the idea of Rückamp *et al.*,[11] who proposed a Landau theory for the incommensurate transition. This phenomenological theory includes the tendency to dimerize of each chain and the coupling of the order parameter with the neighboring chain. As a result the incommensurate phase is accounted. However the sign and the value of the parameters are phenomenologically chosen and the connection with the underlying microscopic theory is not clear.

In view of the previous discussion, in this paper we propose a simplified microscopic model which accounts for the transition from the uniform to the incommensurate phase in TiOCl. Our model contains the relevant magnetic interaction, the phonons and the spin-phonon coupling. The paper is organized as follows. In Sec. II we present the model and show that the essential ingredient leading to the incommensurate transition is that the phononic dispersion of the modes near π is linear. In Sec. III we apply the model to TiOCl. We start by fitting the parameters in order to account for the measured phononic frequencies and the value of the incommensurate wave vector at the transition temperature. After that, we ob-

tain the dynamical structure factor of the phonons and compare it with the one obtained in x-ray experiments. The softening of a phonon and the loss of spectral weight when the transition approaches is correctly accounted.

II. MODEL AND INCOMMENSURATE TRANSITION

We include the Ti atoms on the bilayer structure which interact by harmonic forces as depicted in Fig. 1. For simplicity we consider ionic displacements only in the direction of the magnetic chains. As the measured magnetic susceptibility of TiOCl is well reproduced by a 1D Heisenberg model, we assume that the Ti atoms are magnetically coupled only along the b direction. Moreover, as a direct exchange seems to be the dominant Ti-Ti interaction, we assume that $J(\Delta u)$ is modulated by the movement of nearest-neighbor Ti ions in the chain direction. Our spin-phonon Hamiltonian reads

$$H = H_{\mathrm{ph}} + H_s + H_{\mathrm{sph}},$$

$$H_{\mathrm{ph}} = \sum_{i,j} \frac{P_{i,j}^2}{2m} + \sum_{i,j} \left\{ \frac{K_{\mathrm{in}}}{2}(u_{i,j} - u_{i+1,j})^2 + \frac{K_{\mathrm{inter}}}{2}[(u_{i,j} - u_{i,j+1})^2 + (u_{i,j} - u_{i+1,j-1})^2] \right\},$$

$$H_s = J \sum_{i,j} \mathbf{S}_{i,j} \cdot \mathbf{S}_{i+1,j},$$

$$H_{\mathrm{sph}} = \sum_{i,j} \alpha(u_{i+1,j} - u_{i,j}) \mathbf{S}_{i,j} \cdot \mathbf{S}_{i+1,j}, \tag{1}$$

where $P_{i,j}$ is the momentum of the atom i of the chain j, $u_{i,j}$ are the displacements from the equilibrium positions along the direction b of the magnetic chains, $\mathbf{S}_{i,j}$ are spin-$\frac{1}{2}$ operators with exchange constant $J=J(\Delta u=0)$ along the b axis of a nondeformed underlying lattice, $\alpha=[dJ(\Delta u)/d\Delta u]|_{\Delta u=0}$, and K_{in} and K_{inter} are the in-chain and interchain harmonic force constants as shown in the Fig. 1.

Representing the atom displacements and momenta through phonon normal coordinates, we can write the phonon dependent parts of the Hamiltonian as

$$H_{\mathrm{ph}} = \sum_{\mathbf{q}} \hbar\Omega(\mathbf{q}) \left(a_{\mathbf{q}}^{\dagger} a_{\mathbf{q}} + \tfrac{1}{2} \right),$$

$$H_{\mathrm{sph}} = \frac{1}{\sqrt{N}} \sum_{\mathbf{q}} g(1 - e^{ibq_y}) Q(\mathbf{q}) \sum_{i,j} e^{i\mathbf{q}\cdot\mathbf{R}_{i,j}} \mathbf{S}_{i,j} \cdot \mathbf{S}_{i+1,j},$$

where $\Omega(\mathbf{q})$ is the phonon-dispersion relation which reads

$$\Omega^2(\mathbf{q}) = \frac{4}{M} \left[K_{\mathrm{in}} \sin^2 \frac{q_y}{2} + K_{\mathrm{inter}} \left(1 - \cos\frac{q_x}{2} \cos\frac{q_y}{2} \right) \right], \tag{2}$$

for our model and $g=\frac{\alpha}{\sqrt{M}}$. The quantized phonon normal coordinates are defined by

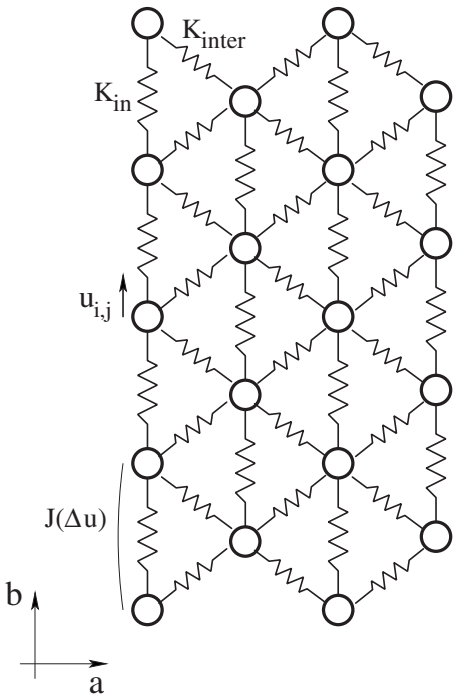

FIG. 1. Schematic representation of our simplified model. Only Ti atoms are included over the ab plane. K_{in} and K_{inter} are the harmonic force constants acting when two neighbor atoms in the same chain and in neighboring chains, respectively, move from their equilibrium position.

$$Q(\mathbf{q}) = \sqrt{\frac{\hbar}{2\Omega(\mathbf{q})}} (a_{-\mathbf{q}}^{\dagger} + a_{\mathbf{q}}).$$

It will be also useful to introduce a dimensionless spin-phonon coupling constant defined as in Ref. 4:

$$\lambda = \frac{4g^2}{\pi J \Omega^2(q_y = \pi)}.$$

To compare with x-ray scattering data, the dynamical structure factor $S(\mathbf{q},\omega)$ has to be determined. It is related to the phononic retarded Green's function[14] by

$$S(\mathbf{q},\omega) = -\frac{\Omega(\mathbf{q})}{\pi} \frac{\mathrm{Im}\ \mathcal{D}^{\mathrm{ret}}(\mathbf{q},\omega)}{1 - e^{\beta\omega}},$$

where

$$\mathcal{D}^{\mathrm{ret}}(\mathbf{q},\omega) = \frac{\mathcal{D}^0(\mathbf{q},\omega + i\delta)}{1 - \mathcal{D}^0(\mathbf{q},\omega + i\delta)\Pi(\mathbf{q},\omega + i\delta)}. \tag{3}$$

$\mathcal{D}^0$ denotes the noninteracting phonon Green's function defined by

$$\mathcal{D}^0(\mathbf{q}, i\omega_n) = \frac{2}{(i\omega_n)^2 - \Omega^2(\mathbf{q})},$$

and $\Pi(\mathbf{q},\omega)=\Pi(q_y,\omega)$ is the phonon self-energy. In the following, we treat the spin-phonon interaction using a random-phase approximation (RPA) for the phonon self-energy term along with the expression obtained by Cross and Fisher[4] us-

ing bosonization for the dimer-dimer correlation function in the Heisenberg model:

$$\Pi(q_y,\omega) = -\frac{0.37}{T}|(1-e^{iq_y b})g|^2 I_1 \times\left(\frac{\omega+\frac{\pi}{2}Jb(q_y-\pi)}{2\pi T}\right)I_1\left(\frac{\omega-\frac{\pi}{2}Jb(q_y-\pi)}{2\pi T}\right),$$

with

$$I_1(k) = \frac{1}{\sqrt{8\pi}}\frac{\Gamma\left(\frac{1}{4}+\frac{1}{2}ik\right)}{\Gamma\left(\frac{3}{4}+\frac{1}{2}ik\right)}.$$

Let us start by identifying the structural transition of the model by searching the poles of the retarded Green's function when $\omega=0$ over the (q_x,q_y) plane of the first Brillouin zone. They are given by the equation of the zeros in the denominator of Eq. (3), which reads

$$\Omega^2(\mathbf{q}) + 2\Pi(q_y,0) = 0. \quad (4)$$

From this equation we obtain $T(\mathbf{q})$, the temperature where the renormalized frequency vanishes for each $\mathbf{q}$. The highest of these temperatures signals the $\boldsymbol{q}$ wave vector of the structure that will be developed at that T. For an isolated chain this transition takes place at $\mathbf{q}=(0,\pi)$, which is the usual spin-Peierls transition toward the dimerized phase.

How does this situation change when the system acquires a transversal dispersion due to an elastic coupling between the chains? Certainly, if the chains arrange in a rectangular geometry (atoms in different chains align in phase), the dispersion of the phonons in the chain direction has a local maximum at $q_y=\pi$ and the $T(\mathbf{q})$ given by Eq. (4) has a maximum at $\mathbf{q}=(0,\pi)$. Thus, no complete softening of an incommensurate mode is found.

A crucial consideration here is that the dispersion given by Eq. (2), when expanded near $q_y=\pi$, reads

$$\Omega^2(\mathbf{q}) \sim \frac{4}{M}\left[K_{\text{in}} + K_{\text{inter}}\left(1-\frac{\delta}{2}\cos\frac{q_x}{2}\right)\right],$$

$$\delta \equiv \pi - q_y,$$

i.e., it increases linearly near π. Plugging this expression into Eq. (4) and expanding up to order δ, we obtain

$$T(\delta) = \frac{g^2 M|a_0|}{K_{\text{inter}}+K_{\text{in}}}\left[1+\frac{1}{2}\frac{K_{\text{inter}}\cos\left(\frac{q_x}{2}\right)\delta}{K_{\text{inter}}+K_{\text{in}}}\right], \quad (5)$$

where it was enough to calculate $\Pi(q_y,0)$ at $q_y=\pi$ as $\Pi(\pi,0)=\frac{2a_0 g^2}{T}$, with $a_0=-0.257\,743$, because the first correction is of second order in δ.

The temperature given in Eq. (5) decreases with q_x and increases for increasing δ. Therefore an instability is predicted at $q_x=0$ and q_y shifted from π. The next orders of $T(\delta)$ stabilize a local maximum at a given δ. Thus, due to the linear dispersion of the relevant phonon mode, model (1) has a transition from a uniform to an incommensurate phase by lowering the temperature. The physical reason why this transition appears in the triangular arrangement and not in the rectangular one is that the elastic energy that the system gains by distorting the lattice in a modulated pattern decreases faster in the first case, when the wave vector of the modulation moves away from π. This reduction overcomes the cost in the magnetic free energy the system should pay to separate from the dimerized state. This reduction does not take place in the rectangular case and the system never goes to an incommensurate phase but directly to a dimerized one.

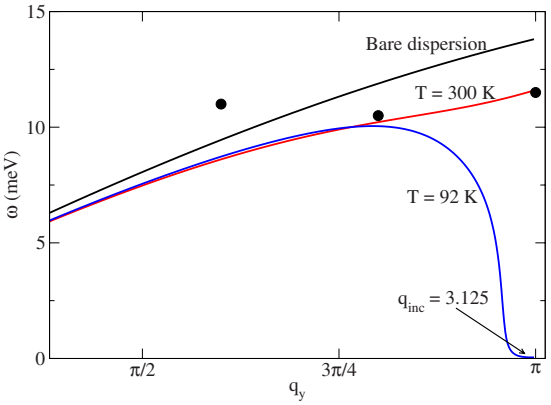

FIG. 2. (Color online) Evolution with the temperature of the dressed frequency of the phonons along the $(0,q_y)$ path. The model parameters are $\sqrt{4K_{\text{in}}/M}=6.6$ meV, $K_{\text{inter}}\sim 3.38K_{\text{in}}$, and $\lambda=0.17$. The black dots are the experimental points obtained by inelastic x-ray scattering at $T=300$ K (Ref. 15).

III. APPLICATION TO TiOCl

Having shown that the uniform-incommensurate transition is present in our model, we will try to fit the parameters to account for the available experimental data of TiOCl. We intend to reproduce the experimental incommensurate wave vector $q_y \simeq 3.04$ (Refs. 15 and 16) and the renormalized frequency of the phonons near the zone boundary at 300 K obtained in Ref. 15 by inelastic x-ray scattering. In order to do that we have to fix the free parameters of our model, i.e., the elastic constants and the spin-phonon coupling. Usually the critical temperature is used to fix the spin-phonon coupling. This value could be obtained by numerical solution of Eq. (4) once the other parameters are known. The values of K_{in} and K_{inter} are fixed in such a way to fit the phononic frequencies measured by inelastic x-ray scattering at $T=300$ K with the ones obtained from the positions of the peaks of $S(q,\omega)$.

The value of the in-chain elastic constant was set to $\Omega_{\text{in}}=\sqrt{4K_{\text{in}}/M}=6.6$ meV and the interchain one was fixed to $K_{\text{inter}}/K_{\text{in}}=3.38$. This enables us to fit the experimental frequencies near $q_y=\pi$ at 300 K with a spin-phonon coupling constant $\lambda=0.17$. The transition temperature is 92 K as in TiOCl. However, using these parameters we obtain an incommensurate wave vector $q_{\text{inc}}=3.125$; i.e., it is close to π and far away from the experimental value. Our results together with the experimental ones are shown in Fig. 2. In this figure we see that as we move away from the zone boundary, the dispersion curve quickly decreases and separates from

the experimental points. Moreover, the bare dispersion curve is very close to the 300 K one.

We have obtained a quite small value of the incommensuration with those parameters. Therefore, in order to reproduce the experimental one, we increase the spin-phonon coupling λ. The new value turns out to be $\lambda=0.41$. This change has the undesired effect of increasing the transition temperature up to $T_{\mathrm{inc}}\sim 225$ K, more than twice the experimental transition temperature. Moreover, if we want to keep adjusting the experimental x-ray phonons at 300 K, we have to increase the value of the bare phonon frequency because of the larger spin-phonon coupling. The chosen values are $\sqrt{4K_{\mathrm{in}}/M}=10.5$ meV and $K_{\mathrm{inter}}\sim 3.38K_{\mathrm{in}}$; i.e., we have kept the ratio $K_{\mathrm{inter}}/K_{\mathrm{in}}$ unchanged. The results are shown in Fig. 3.

Now we see that the calculated 300 K curve does not fall rapidly as before and that the experimental point which is the most separated from the zone boundary is also well adjusted. Nevertheless, we have noted that with this set of parameters the transition temperature is overestimated. This problem is also present in the calculations of Abel *et al.*[15] through an underestimation of the magnetic coupling J. We think that this disagreement is due to the adiabatic treatment of the phonons and will be solved by an extension of the results of Ref. 6 for the geometry of TiOCl. In this paper it was shown that a theory going beyond the mean-field RPA treatment of the phonons by including nonadiabatic effects predicts a reduction in the critical temperature for a given λ. We plan to undertake this generalization in a forthcoming paper, but let us make a rough estimation of the renormalization of the transition temperature using formula (35) of Ref. 6. Note that the parameter Ω_{inter} in Ref. 6 is not exactly the same as in the present paper. It is in this sense that the following results should be taken as an estimation. Proceeding in this way we obtain

$$T = T_{ad}\left(1 - \frac{1}{\sqrt{1+(\Omega_{\mathrm{inter}}/\Omega_{\mathrm{in}})^2}}\right) = 117 \text{ K},$$

where $T_{ad}=225$ K is the transition temperature obtained by the adiabatic approach. The transition temperature given by

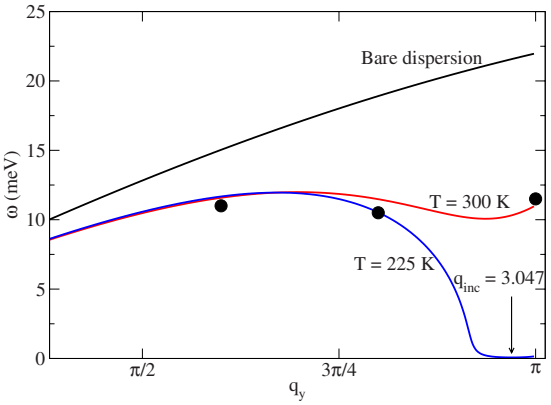

FIG. 3. (Color online) Evolution with the temperature of the dressed frequency of the phonons along the $(0,q_y)$ path. The curves were obtained from the positions of the peaks of the dynamical structure factor. The fitted parameters are $\sqrt{4K_{\mathrm{in}}/M}=10.5$ meV, $K_{\mathrm{inter}}\sim 3.38K_{\mathrm{in}}$, and $\lambda=0.41$.

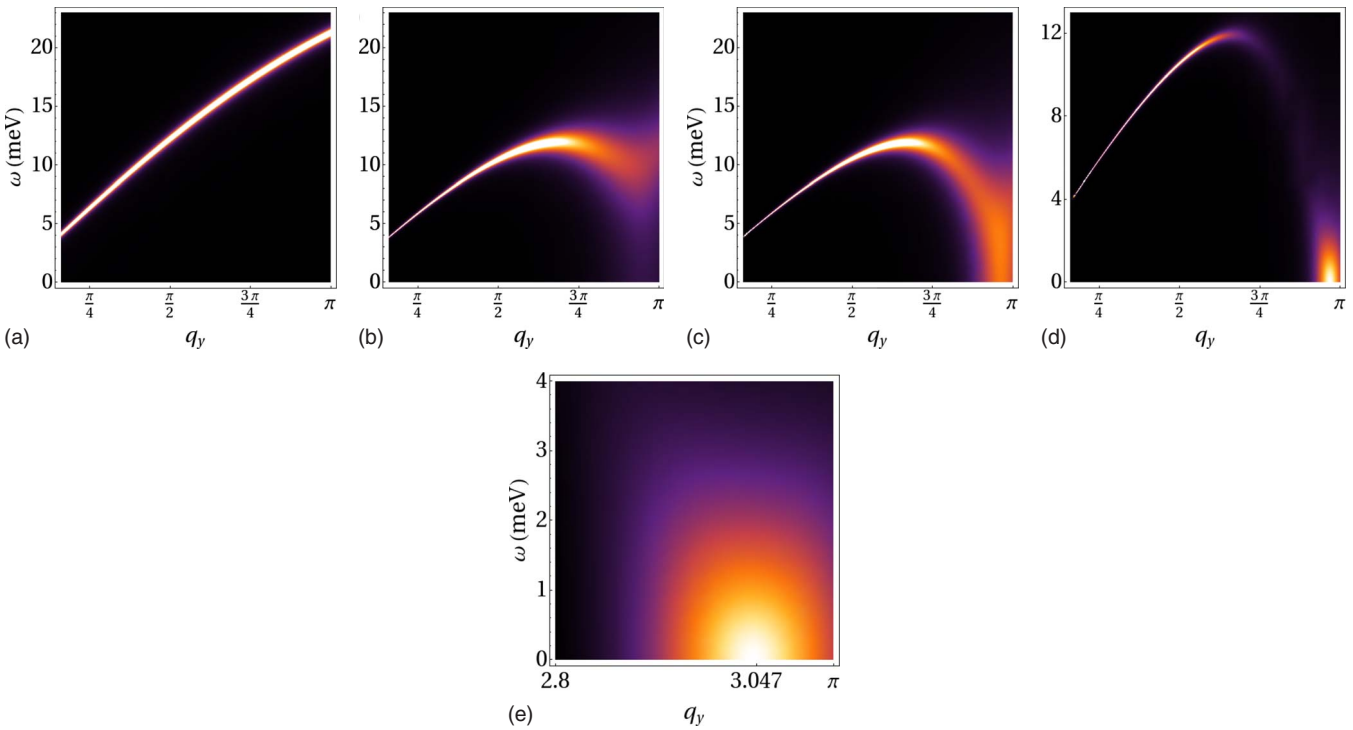

FIG. 4. (Color online) Contour curves of the dynamical structure factor as a function of q_y ($q_x=0$) and ω for different temperatures: (a) 1000, (b) 300, (c) 255, and (d) 225 K (transition temperature). In (e) we show a zoom of (d) around the transition point. Brighter zones correspond to higher intensities. We see that there is a softening of a group of modes near the zone boundary. In this region, there is a broadening of the peak width with decreasing temperature due to a redistribution of the spectral weight.

the nonadiabatic approach is now very close to the experimental one. Furthermore, let us estimate the energy gap by combining Eqs. (26) and (32) of Ref. 6,

$$\Delta = 3.04\lambda J\left(1 - \frac{1}{\sqrt{1 + (\Omega_{\text{inter}}/\Omega_{\text{in}})^2}}\right) = 427.76 \text{ K},$$

i.e., we obtain excellent agreement with the experimental gap of 430 K.[10] From these estimations it can be inferred that the nonadiabatic treatment should solve the problem.

For the present purpose, let us use the second set of parameters. In Fig. 4 we show a plot of the dynamical structure factor along the $(0,q_y)$ path of the first Brillouin zone for a range of frequencies and different temperatures.

When the temperature is high [Fig. 4(a)], we obtain peaks which reproduce the bare dispersion relation of the model. With decreasing temperatures [Figs. 4(b)–4(d)], we observe the trace of the phonon softening along with a broadening and a height reduction of the peak. This is due to a redistribution of the spectral weight which is concentrated again in a defined peak at the transition temperature for $\omega=0$ and $q_y=3.047$ [Fig. 4(d) and zoom in Fig. 4(e)]. This broadening of the peak indicates that phonons are overdamped by the interaction with the magnetic excitations. This behavior was indeed observed experimentally in Ref. 15 [see Fig. 9(b) of this reference] and considered there as a disagreement with the Cross-Fisher theory. Instead, our results show that due to the interaction of the bare phonons with the two-spinon continuum of the magnetic subsystem, the dynamical structure factor of the phonons does not show a Lorentzian character. It is indeed asymmetrical toward low frequencies (Fig. 5). This behavior should be checked in future experiments.

It was recently proposed, from an *ab initio* density-functional theory (DFT), that a weak *ferromagnetic* interchain coupling could be the origin of the incommensuration in this compound.[17] As no quantitative estimation of the incommensurate wave vector has been done, we cannot compare the relative importance of each mechanism. Moreover, the actual values and the signs of the interchain exchanges remain as a controversial question and the results of the present work show that the elastic frustration in the interchain coupling is enough to produce the incommensurate phase.

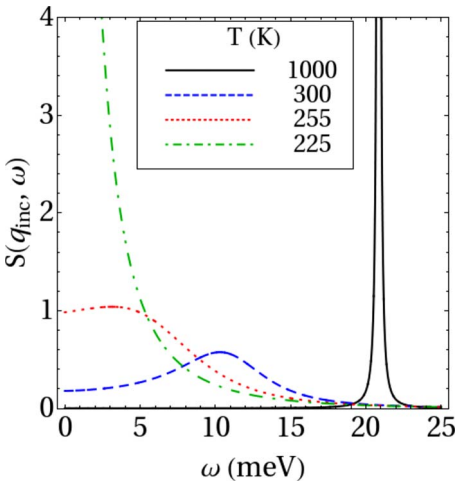

FIG. 5. (Color online) Dynamical structure factor at q_{inc} for different temperatures. At high T, we see a very definite peak which broadens and gets asymmetrical as temperature decreases. At $T=225$ K (the transition temperature), we observe the divergence of the peak for $\omega=0$.

IV. SUMMARY

In this paper we have developed a model which explains the uniform-incommensurate transition in TiOCl. It is based on the competition between the tendency of isolated antiferromagnetic chains to dimerize and the frustrated elastic interchain coupling. The model predicts the softening of an incommensurate mode. Moreover, it is in agreement with the loss of a coherent spectral weight for the phonons near the zone boundary as observed by inelastic x-ray scattering.

ACKNOWLEDGMENT

This work was supported by ANPCyT (Grant No. PICT 1647), Argentina.

[1] R. E. Peierls, *Quantum Theory of Solids* (R. E. Peierls/Oxford University Press, New York, 1955).
[2] J. W. Bray, L. V. Interrante, I. S. Jacobs, and J. C. Bonner, in *Extended Linear Chain Compounds*, edited by J. S. Miller (Plenum, New York, 1983), Vol. 3, pp. 353–415.
[3] G. S. Uhrig, Phys. Rev. B **57**, R14004 (1998).
[4] M. C. Cross and D. S. Fisher, Phys. Rev. B **19**, 402 (1979).
[5] C. Gros and R. Werner, Phys. Rev. B **58**, R14677 (1998).
[6] A. O. Dobry, D. C. Cabra, and G. L. Rossini, Phys. Rev. B **75**, 045122 (2007).
[7] R. Beynon and J. Wilson, J. Phys.: Condens. Matter **5**, 1983 (1993).
[8] M. Shaz, S. van Smaalen, L. Palatinus, M. Hoinkis, M. Klemm, S. Horn, and R. Claessen, Phys. Rev. B **71**, 100405(R) (2005).
[9] A. Seidel, C. A. Marianetti, F. C. Chou, G. Ceder, and P. A. Lee, Phys. Rev. B **67**, 020405(R) (2003).
[10] T. Imai and F. C. Chou, arXiv:cond-mat/0301425 (unpublished).
[11] R. Rückamp, J. Baier, M. Kriener, M. W. Haverkort, T. Lorenz, G. S. Uhrig, L. Jongen, A. Möller, G. Meyer, and M. Grüninger, Phys. Rev. Lett. **95**, 097203 (2005).
[12] A. Schönleber, G. Shcheka, and S. van Smaalen, Phys. Rev. B **77**, 094117 (2008).
[13] D. Fausti, T. T. A. Lummen, C. Angelescu, R. Macovez, J. Luzon, R. Broer, P. Rudolf, P. H. M. van Loosdrecht, N. Tristan, B. Büchner, S. van Smaalen, A. Möller, G. Meyer, and T. Taetz, Phys. Rev. B **75**, 245114 (2007).
[14] G. D. Mahan, *Many Particle Physics* (Plenum, New York, 2000).

[15] E. T. Abel, K. Matan, F. C. Chou, E. D. Isaacs, D. E. Moncton, H. Sinn, A. Alatas, and Y. S. Lee, Phys. Rev. B **76**, 214304 (2007).
[16] A. Krimmel, J. Strempfer, B. Bohnenbuck, B. Keimer, M. Hoinkis, M. Klemm, S. Horn, A. Loidl, M. Sing, R. Claessen, and M. v. Zimmermann, Phys. Rev. B **73**, 172413 (2006).
[17] Y. Z. Zhang, H. O. Jeschke, and R. Valenti, Phys. Rev. B **78**, 205104 (2008).